agriculture

MDPI

Article

Cropland Expansion Mitigates the Supply and Demand Deficit for Carbon Sequestration Service under Different Scenarios in the Future—The Case of Xinjiang

Mingjie Shi [1,2,3], Hongqi Wu [1,2,*], Pingan Jiang [1,2,*], Wenjiao Shi [3,4], Mo Zhang [3,4], Lina Zhang [1,2], Haoyu Zhang [5], Xin Fan [6,7], Zhuo Liu [1,2], Kai Zheng [1,2], Tong Dong [8] and Muhammad Fahad Baqa [4,9]

1 College of Resources and Environment, Xinjiang Agricultural University, Urumqi 830052, China
2 Xinjiang Key Laboratory of Soil and Plant Ecological Processes, Xinjiang Agricultural University, Urumqi 830052, China
3 Key Laboratory of Land Surface Pattern and Simulation, Institute of Geographic Sciences and Natural Resources Research, Chinese Academy of Sciences, Beijing 100101, China
4 College of Resources and Environment, University of Chinese Academy of Sciences, Beijing 100049, China
5 College of Geography and Remote Sensing Sciences, Xinjiang University, Urumqi 830046, China
6 School of Public Administration, China University of Geosciences (Wuhan), Wuhan 430074, China
7 Center for Turkmenistan Studies, China University of Geosciences, Wuhan 430074, China
8 Key Laboratory of Coastal Science and Integrated Management, First Institute of Oceanography, Ministry of Natural Resources, Qingdao 266061, China
9 Key Laboratory of Digital Earth Sciences, Aerospace Information Research Institute, Chinese Academy of Sciences, Beijing 100094, China
* Correspondence: whq@xjau.edu.cn (H.W.); xjaudbxb@xjau.edu.cn (P.J.)

Citation: Shi, M.; Wu, H.; Jiang, P.; Shi, W.; Zhang, M.; Zhang, L.; Zhang, H.; Fan, X.; Liu, Z.; Zheng, K.; et al. Cropland Expansion Mitigates the Supply and Demand Deficit for Carbon Sequestration Service under Different Scenarios in the Future—The Case of Xinjiang. *Agriculture* **2022**, *12*, 1182. https://doi.org/10.3390/agriculture12081182

Academic Editor: María Martínez-Mena

Received: 16 June 2022
Accepted: 4 August 2022
Published: 9 August 2022

Abstract: China's double carbon initiative faces huge challenges, and understanding the carbon sequestration service of terrestrial ecosystems under future interannual regional land use change is important to respond to China's carbon policy effectively. Previous studies have recognized the important impact of land use/land cover (LULC) planning on carbon sequestration in terrestrial ecosystem services (ESs). However, exploring trends in carbon sequestration under sustainable development scenarios that combine economic and ecological development, particularly the mechanisms that balance the supply and demand of carbon sequestration, still requires in-depth exploration in different geographical contexts. In this study, we present the LULC simulation framework from 2000 to 2030 for four different development scenarios in the Xinjiang region, located in an important Belt and Road region, including business as usual (BAU), rapid economic development (RED), ecological land protection (ELP), and sustainable development with both economic and ecological development (SD). Our results suggest that both the supply and demand of carbon stock in Xinjiang will increase in 2025 and 2030, with the demand exceeding the supply. However, our scenario planning mitigates the supply and demand deficit situation for carbon sequestration in the context of future cropland expansion in different scenarios. In summary, our study's findings will enrich the study of carbon sequestration under future scenarios in the Belt and Road region. Xinjiang should pay more attention to the dynamic changes in landscape type structure and its carbon storage supply and demand caused by cultivated land expansion. Among the four scenarios, the spatial difference between carbon storage supply and demand based on the SD scenario is the smallest, which is more in line with the high-quality development of regional ecological security in Xinjiang.

Keywords: carbon sequestration; different scenarios; land use; sustainable development; Xinjiang

1. Introduction

Along with the Chinese government's goal of achieving peak carbon by 2030 and carbon neutrality by 2060, the timely assessment of the terrestrial ecosystem carbon sequestration service has become one of the most important issues in response to the current carbon neutrality policy [1]. As the paramount indicator of ecosystem carbon stock services, terrestrial ecosystem carbon sequestration is critical to the carbon cycle [2–4]. Land use/land cover (LULC) change is one of the major factors influencing carbon sequestration in terrestrial ecosystems, as land use changes affect the material cycling and energy flow of soils and vegetation carbon sequestration by altering the structure and function of the original ecosystem [5]. Most studies only consider the supply of ecosystem services, ignoring the human demand for ecosystem services [6,7]. Therefore, exploring the coupling of supply and demand in terrestrial ecosystem carbon sequestration is crucial to deepening future human, economic, and social knowledge of carbon source sinks.

The methods currently used to assess carbon sequestration at national and regional scales fall into three broad categories [4,8,9]. The first is the field survey method, which is primarily an area-weighted average method based on soil profiles [3]. However, this type of study may cause some multi-scale variation in results due to differences in soil profile size, location, methods, and sampling periods [10]. The second approach is empirical biogeochemical modeling [11,12]. This approach creates much uncertainty in assessing carbon sequestration, mainly due to differences in the mechanisms or structures of different models [10]. Third are remote sensing methods for calculating net primary production (NPP) which are often used to estimate carbon stocks, but they produce very large errors in some arid and semi-arid regions [13,14]; further, using spatial scales smaller than NPP, typically <1 km resolution, does not provide a true per-pixel NPP output [15]. Currently, the combination of land use and terrestrial ecosystem carbon stock models is widely used in studies to estimate carbon sequestration and their future spatial variability, and the application of such methods is an important trend concerning the development of dynamic carbon stock assessments for the future [12,16]. Among the many models quantifying the carbon sequestration of ecosystem services, machine learning is considered a feasible and reliable method for assessing carbon sequestration, and it has been widely used in carbon stock assessments at national and regional scales to balance overexploitation and environmental protection [8,17]. However, there are still some limitations to the abovementioned research methods. First, they fail to analyze carbon sequestration under different future scenarios, and only assess current carbon sequestration in a single way. Secondly, it has not been possible to explore the coupling between the supply and demand of carbon sequestration in terrestrial ecosystems. Third, they fail to address the deficit in the supply and demand of carbon sinks resulting from the expansion of cropland under different future scenarios. Therefore, it is important to explore the coupling between the supply and demand of carbon sequestration under different future LULC policy scenarios for planning and analyzing the surplus/deficit of carbon sequestration in the context of cropland expansion to provide a balance of supply and demand for a sustainable landscape pattern.

While there is growing recognition of the impacts of rapid LULC change due to urbanization on ecosystem services (ESs), the LULC landscape continues to be transformed in an unsustainable manner [18]. Land management is one of the most important factors influencing land cover, either directly or indirectly, with policy and environmental planning decisions having a significant impact on how land is managed [19]. Moreover, at the landscape level, the current main challenge is to identify alternative best management scenarios for different LULC change scenarios [9]. Numerous studies have shown that the environmental impact could be improved by changing LULC dynamics [20–23]. For example, a study conducted in Hawaii, USA, examined various LULC scenarios, with an increase in the carbon sequestration service of 3458 tons of carbon in each specific scenario [20]. Research in the Willamette Basin of Oregon has shown that different scenarios of LULC can influence the spatial pattern of the carbon sequestration service and that optimized scenarios can increase carbon sequestration in terrestrial ecosystems [21]. Furthermore, a study in Beijing–Tianjin–Hebei, China, planned four different scenarios to explore the maximum area of ESs loss, thus ensuring that the critical ESs are not affected [22]. However, while previous studies have explored carbon sequestration from the perspective of maximizing economic or ecological benefits [21], there is still a paucity of studies that have examined the targeting of sustainable development goals (SDGs) for assessing carbon sequestration under sustainability scenarios that combine economic and ecological development.

The UN Sustainable Development Goals (SDGs) focus on regional development and ecological security. In the context of the SDGs, it is important to understand regional sustainable development planning and to assess local ecological security [24]. To fill the above research gaps, this paper takes the Xinjiang Uyghur Autonomous Region (hereinafter referred to as Xinjiang) as the study area, because this core area of the Silk Road along the Belt and Road can better reveal the spatial distribution characteristics and evolutionary patterns of mountain ecosystems in a temperate arid zone [25,26]. The study uses the gray multi-objective optimization–patch generation land use simulation (GMOP-PLUS) model to simulate the variation in land use landscape patterns under various scenarios and propose a sustainable development scenario that balances economic and ecological development. The study further applies a random forest model to quantify the carbon sequestration of terrestrial ecosystems in Xinjiang under different scenarios from 2000 to 2030 and to explore the coupling between the supply and demand of carbon sequestration. The main objectives of this study are three-fold: (i) to predict spatial–temporal patterns of land use in Xinjiang from 2020 to 2030 by the PLUS model under the business as usual, rapid economic development, ecological land protection, and sustainable development scenario; (ii) to quantify the spatial and temporal variation characteristics of terrestrial ecosystem carbon sequestration under different scenarios in Xinjiang during 2020–2030 using random forest models; and (iii) to elucidate the relationship between the supply and demand of carbon sequestration in Xinjiang, and explore the difference between the supply and demand of LULC on carbon sequestration under different scenarios.

2. Materials and Methods

2.1. Study Area

Xinjiang is located inland in northwestern China, with a geographical location bounded by (73°40′~96°18′ E, 34°25′~48°10′ N), spanning 2000 km from east to west and 1650 km from north to south, with an area of about 1.66×10^6 km^2, this accounting for about one-sixth of China's land area (Figure 1). The average annual temperature in Xinjiang is 10.5 °C, and there is ca. 2600 h of sunshine per year. The average annual rainfall is 145.5 mm, and the average annual evaporation is 1000–4500 mm.

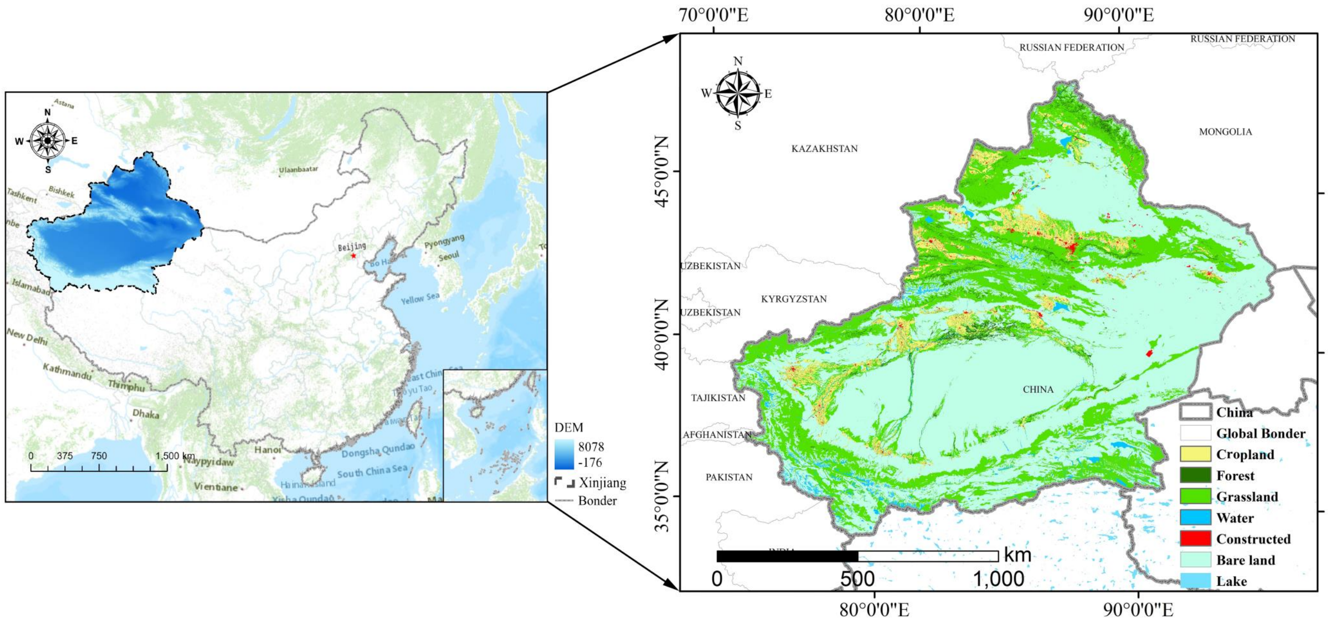

Figure 1. Digital elevation model of the study area.

As the core region of the overland Silk Road Economic Belt, Xinjiang is an important link for political, economic, and cultural exchanges between China and other Belt and Road countries. The Xinjiang government has historically attached importance to the multiple roles played by ecological and environmental protection, enacting and implementing several master land use plans in conjunction with an ecologically sustainable development agenda. Quantifying green spatial patterns and exploring trends in green spatial change in Xinjiang are essential for assessing and mapping the mismatch between supply and demand for ESs and providing guidance for future landscape and urban planning [25].

2.2. Data and Processing

The LULC dataset used in the study mainly includes: (1) Five periods of land use data with a spatial resolution of 30 m for 2000, 2005, 2010, 2015, and 2020 from the CAS Data Centre for Resource and Environmental Sciences (http://www.resdc.cn, (accessed on: 15 June 2022)). All these data were combined with field surveys, visual interpretation, and confusion matrix judgment, allowing for the total accuracy of the interpretation to reach 94.3% and the total accuracy of the 25 sub-categories to reach 91.2% [27]. According to the national land use category 1 classification system, there are six types of land: cropland, forest land, grassland, construction land, bare land, and water. (2) The annual average temperature and precipitation data used to discern suitability conditions for different land types were obtained from the CAS Data Centre (http://www.resdc.cn (accessed on: 15 June 2022)). For the latest year of meteorological data, we obtained raster data at a 250 m resolution by spatial interpolating the annual average data for 2020 from meteorological stations. (3) Digital elevation model (DEM) data, used to drive the LULC simulations for natural environmental factors, were obtained from the Geospatial Data Cloud (http://www.gscloud.cn (accessed on: 15 June 2022)) at a spatial resolution of 30 m. Soil type raster data came from the FAO dataset of the Food and Agriculture Organization of the United Nations (https://www.fao.org, (accessed on: 15 June 2022)). (4) Socioeconomic data, mainly containing the spatial distribution of population and gross domestic product (GDP) 1 km gridded data, came from the CAS Data Centre (http://www.resdc.cn (accessed on: 15 June 2022)). Vector datasets for assessing the distance to major roads and the distance to secondary roads came from Open Street Map (http://www.openstreetmap.org (accessed on: 15 June 2022)), and the vector data for river systems came from the National Geographic Information Resource Service (http://www.webmap.cn (accessed on 15 June 2022)). Urban night lighting data were obtained from the China Research Data Service Platform (https://www.cnrds.com (accessed on: 15 June 2022)). (5) The carbon density data of China's terrestrial ecosystems were taken from papers published between 2004 and 2014 and coupled with relevant experimental data from the same time period to generate a complete, systematic database of China's vegetation and soil organic carbon density [28]. In addition, all raster data were resampled to a spatial resolution of 250 m.

2.3. The GMOP-PLUS Model

2.3.1. PLUS

To better understand, assess, and predict future land use changes, research scholars have developed numerous land use simulation models. However, such models are usually linear and numerically based and cannot simulate all land use change processes [29]. However, the PLUS model can make use of the rule mining framework of the land expansion analysis strategy (LEAS) to yield a higher simulation accuracy than other models and better portray the landscape patterns of different future scenarios [25,29].

Under the influence of human social activities and regional socio-economic development, both the natural environment and policy factors can promote certain land use. Natural environmental factors include temperature and precipitation, among others. The process by which they drive such changes is complex and relatively stable, and the ensuing change is often small in magnitude over a short period. Policy factors that affect land use changes include GDP and population. In this paper, 12 driving factors affecting land change are used to reflect the changes of regional ecological environment and provide guidance and reference for the future planning of local land use [9,25,29].

To simulate the patch evolution of different scenarios of land use types, a multi-type random patch seeding mechanism based on threshold descent was used in the PLUS model:

$$OP_{i,k}^{1,t} = \begin{cases} P_{i,k}^{1} \times (r \times \mu_k) \times D_k^t & if\ \Omega_{i,k}^t = 0\ and\ r < P_{i,k}^1 \\ P_{i,k}^{1} \times \Omega_{i,k}^t \times D_k^t & all\ others \end{cases}, \tag{1}$$

where r is a random value in the range 0–1 and μ_k is the threshold value for generating new land-use patches of land use type k. The land use type k can be used to generate new land use patches. The number of decision trees is 50, the sampling rate is 0.01, and the number of features used to train the random forest is 12 (i.e., the same as the number of drivers) [29].

2.3.2. Gray Multi-Objective Optimization (GMOP)

GMOP is a dynamic multi-objective planning method that searches for ways to optimize the use of land given a variety of constraints imposed by different scenarios. It also takes into account the uncertainty of those constraints [30]. Accordingly, it is better able to make accurate models of how land use is spread out in space. The goal of this study was to find a sustainable way to use land with GMOP by using the objective optimization functions, constraints, and parameters that have been suggested by other studies [29,31].

2.3.3. GMOP-PLUS

Having been developed from the GM model and gray theory combined with multiple objectives, GMOP can consider the uncertainty of future LULC occurrence and solve the optimization problem of LULC by handling multiple constraints [32]. Previous studies have shown that the GMOP coupled PLUS model can play a comprehensive and decisive role in directing policy concerning the spatial allocation of land use [29,31]. Hence, the sustainable development scenario projected in this paper goes a step further than those used in previous studies [31,32]. In addition, we used Lingo 12.0 software to predict the spatial quantitative changes to the SD scenario in 2025 and 2030.

In our study, the land use structure of the SD scenario is assumed to maximize all three objectives simultaneously (Table 2) [30]. That is, with (1) $max_{E_{d(x)}}$ to maximize economic benefits, and (2) $max_{E_{p(x)}}$ to maximize ecological benefits, GMOP's optimization objectives are as follows:

$$E_{d(x)} = \sum_{i=1}^{n} d_i \cdot x_i, \tag{2}$$

$$E_{p(x)} = \sum_{i=1}^{n} p_i \cdot x_i\ . \tag{3}$$

where $E_{d(x)}$ and $E_{p(x)}$ denote economic and ecological benefits, respectively; x_i denotes the i category of land variable (i = 1, 2, . . . , 6); and d_i and p_i are the coefficients of economic and ecological benefits of the land category per unit area, respectively.

Table 1. Constraints on the objective function for the 2025 SD scenario (and likewise for 2030).

Subject to (Unit: Pixel Number)	Description
$x_1 + x_2 + x_3 + x_4 + x_5 + x_6 = 26{,}214{,}249$	The sum of the total area of all land use types generally remained constant before and after the simulation.
$1{,}384{,}334 \leq x_1 \leq 1{,}507{,}440$	To guarantee regional food security, the cropland area should not be lower than the 2020 level and less than the maximum number of pixels in the three scenarios (BAU, RED, and ELP).

Table 2. Constraints on the objective function for the 2025 SD scenario (and likewise for 2030).

Subject to (Unit: Pixel Number)	Description
$436,000 \leq x_2 \leq 448,145$	Forest is the ecological barrier of Xinjiang and should not be less than the 2020 level and less than the maximum number of pixels in the three scenarios (BAU, RED, and ELP).
$7,685,687 \leq x_3 \leq 7,851,922$	Grassland can contribute to livestock development, soil and water conservation, and ecological balance and should not be less than the 2020 level, and less than the maximum number of pixels in the three scenarios (BAU, RED, and ELP).
$539,509 \leq x_4 \leq 5,664,23$	The water area should be at least 90% of the 2020 level and less than the maximum number of pixels in the three scenarios (BAU, RED, and ELP).
$149,029 \leq x_5 \leq 153,558$	With the steady development of Xinjiang, which is bound to attract more people, the constructed area should be no less than the 2020 level and less than the maximum number of pixels in the three scenarios (BAU, RED, and ELP).
$15,761,239 \leq x_6 \leq 15,841,522$	We set the area of bare land to be greater than the 2020 level and below the maximum number of pixels in the three scenarios (BAU, RED, and ELP).

Achieving an optimal land use structure requires maximizing both objectives:

$$max\{E_{d(x)}, E_{p(x)}\} \tag{4}$$

2.4. Scenario Setting and Land Use Requirements

2.4.1. Scenario Setting

The research can be broadly divided into the following three steps. First, data on the LULC and the various drivers were prepared, and transformation rules for the LULC were developed. Second, spatial optimization of future LULC was carried out based on the PLUS model and Markov chain, and four different development scenarios were planned and simulated. Third, we explored the supply and demand balance relationships of the carbon sequestration service in Xinjiang terrestrial ecosystems under the different scenarios (Figure 2).

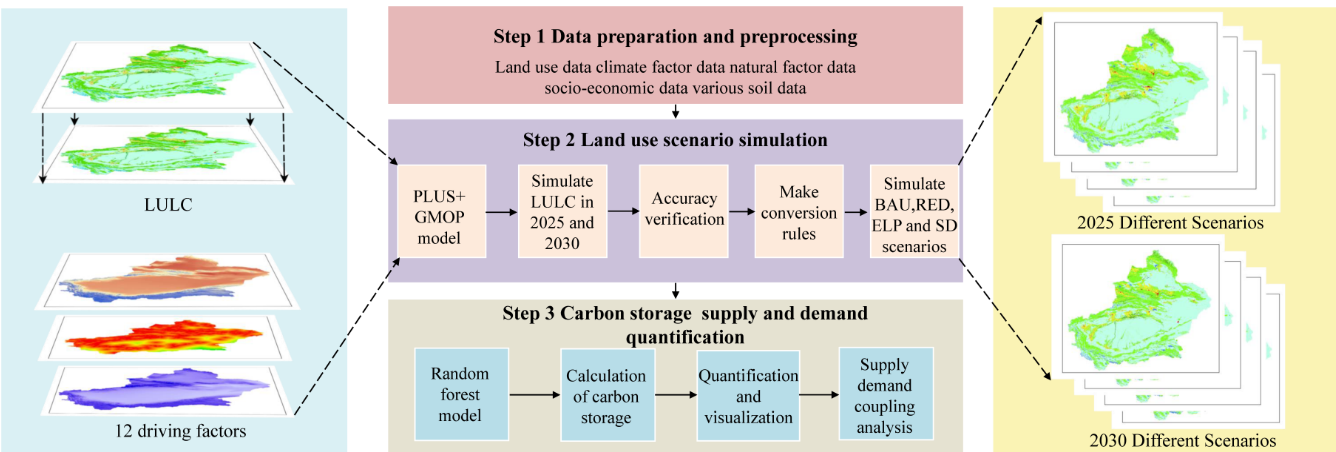

Figure 2. Science–policy framework linking institutional and ecological information.

Four alternative potential land use change scenarios are presented in this study, namely the business as usual (BAU), rapid economic development (RED), ecological land protection (ELP), and sustainable development (SD) scenarios. The principles and objectives of the design scenarios are as follows:

1. BAU scenario: This scenario assumes that land use change trends from the past will continue and that land demand for the BAU year of 2025 will be calculated based on the transition probability of shifts in the Markov chain for the 2015–2020 period and the 2030 BAU year based on the transition probability of shifts in the Markov chain for 2020–2025 BAU [9,25].
2. RED scenario: This scenario is based on the policy of rapid development of urban construction land in the region of the General Land Use Plan of the Xinjiang Uygur Autonomous Region [25]. The RED scenario prioritizes rapid economic development, leading to more demand for urban space. Based on the BAU scenario, and through a combination of thresholds set by previous studies, expert opinions, etc., we assume that the RED scenario accelerates the rate of conversion of grassland, construction land, and bare land to cropland by 50% and that the rate of conversion of cropland, grassland, and water to built-up land increases by the same 50% [33].
3. ELP scenario: This scenario is based on the Grain for Green Project, the Three-North Shelter Forest Program (TNSFP), and the 14th Five-Year Plan for Ecological Protection and represents the strengthening of the local government's commitment to forestry. This scenario represents the execution of the local government's policy of strengthening the protection of forests, grasslands, and water sources, strictly controlling the growth of cropland and construction land, and encouraging the return of farmland to forests, grass, and lakes. In this scenario, we modify the development potential of the cropland layer to convert farmland with a slope between 6° and 25° into grassland, and farmland with a slope greater than 25° into woodland. In addition, a buffer zone of 100 m near river waters was established as a woodland–grassland buffer zone [34].
4. SD scenario: The first three scenarios are more extreme, but the future development of Xinjiang cannot necessarily be modeled using a single scenario, and a trade-off between the three scenarios is needed to find the most appropriate development model for the region. To this end, this study proposes a sustainable development (SD) scenario, which provides a perspective on the trade-offs between the three scenarios. SDGs 15.3.1 represents the proportion of total land area that is degraded, which is a combination of three sub-indicators: land use change, land productivity, and carbon sequestration above and below ground. Given the data availability in our study, we have simplified the SDG 15.3.1 scenario by using only the land use scenario [35]. Although the SDG 15.3.1 scenario calculated here may not sufficiently reflect future realities, using GMOP-PLUS results to characterize the SDGs may provide a new perspective for planning SDGs under future land use change scenarios. Most importantly, specific implementation data for the SDGs model are not yet available for individual countries [36].

2.4.2. SD Scenario Setting

This study uses the GMOP-PLUS model to simplify the SD scenario not only to protect, restore, and promote the sustainability of terrestrial ecosystems, but also to account for rapid economic development. We first set up the land use economic value indicators to parameterize the individual land categories in the land use data. Here, x_1 = cropland; x_2 = forest; x_3 = grassland; x_4 = water; x_5 = construction; and x_6 = bare land. The average land economic value (RMB/hm^2) of each land category can be obtained from the Xinjiang Government Work Report and the Xinjiang 2020 Statistical Yearbook [30,37], and finally the economic value indicator formula was obtained as follows:

$$E_{red(x)} = 2.8x_1 + 0.22x_2 + 0.16x_3 + 0.08x_4 + 85.52x_5 + 0x_6 \tag{5}$$

Setting the ecological value index of land use, through the Xinjiang government work report and previous research results [31,37,38], the ecological value per unit area of land use (RMB/hm^2) was obtained, and the ecological value index formula was obtained as follows:

$$E_{elp(x)} = 1.31x_1 + 7.83x_2 + 2.57x_3 + 35.80x_4 + 0.0082x_5 + 0.016x_6 \quad (6)$$

To achieve the optimal sustainability scenario, the land use structure needs to maximize both of these indicators so that $E_{sdgs(x)}$ reaches the optimal ratio:

$$E_{sdgs(x)} = max\{E_{d(x)}, E_{p(x)}\} = \alpha E_{red(x)} + \beta E_{elp(x)} \quad (7)$$

The optimal adjustment of the land use structure should be designed according to the actual development of the region with a variety of structural optimization and adjustment options to be considered for positioning Xinjiang's development in the next five years with the simultaneous enhancement of economic and ecological benefits.

2.5. Carbon Sequestration Service Supply and Demand

2.5.1. Carbon Sequestration Service Supply

In this study, we chose the random forest (RF) model to estimate the spatial and temporal dynamics of carbon sequestration in Xinjiang [17,39]. RF is an ensemble of decision tree predictors that uses bootstrap resampling methods to build decision trees for each sample [39,40]. For the construction of each tree, samples were selected independently; however, the distribution of all decision trees in the forest is the same, which guarantees the robustness of the model. The advantage of random forest is that it can prevent the overfitting of data, and it is favored for its relatively high overall accuracy and Kappa coefficient, interpretability of results, and accuracy of spatial display results for soil carbon sequestration prediction. The RF model is available in the Random Forest R 4.1.2 package. In this study, we divided the carbon sequestration of terrestrial ecosystems into three carbon pools: aboveground biomass carbon pool, underground biomass carbon pool, and soil carbon pool (0–20 cm). RF was used to model these three data parts separately and then add them together.

The carbon density data for this study were obtained from an open access database of the Chinese Academy of Sciences [28,41]. This is a publicly available carbon density dataset that includes 3026 soil samples taken from the soil surface layer across China through 2014. These samples were obtained from 1036 published papers and field survey data. The number of points in Xinjiang is 231, which covers its six major land use types. Thus, this database could provide new insights for future carbon sequestration strategies in Xinjiang. Because the data for dead organic carbon is relatively complex and difficult to observe and obtain, only carbon stored aboveground, belowground, and in the soil was considered in this study [28]. The model was calculated as follows:

$$C_{cs} = C_{i-above} + C_{i-below} + C_{i-soil} \quad (8)$$

$$C_{stocks} = C_{0-20} \times AREA_i \quad (9)$$

where C_{CS} is the carbon density; $C_{i-above}$ is the carbon density of the aboveground plant biomass, kg/m^2; $C_{i-below}$ is the carbon density of belowground biomass of plant roots, kg/m^2; and C_{i-soil} refers to the density of soil organic carbon in the soil layer, kg/m^2. C_{stocks} is the total carbon sequestration and $AREA_i$ denotes the area of different land use types or soil types.

2.5.2. Carbon Sequestration Service Demand

The demand for carbon sequestration service was estimated as the difference between the actual carbon emissions and the allowable carbon dioxide emissions set by local governments, as per Equation (10), consistent with previous research [27]. For spatial mapping, the amount of carbon emissions from industry was split evenly between construction, grassland, woodland, and cropland. The demand for carbon sinks from personal energy was split evenly across construction land:

$$D_{CS} = E_{industry} + E_{transportation} + E_{living} \tag{10}$$

where D_{CS} is the carbon sequestration demand; $E_{industry}$, $E_{transportation}$, and E_{living} are the carbon emission data of industry, transportation, and personal energy, respectively; $E_{industry}$ is the amount of carbon dioxide released by industrial production, whose value comes from the Xinjiang Statistical Yearbook; and $E_{transportation}$ is the carbon emitted by transportation. Each car uses about 1564.9 kg of gasoline per year, and one vehicle in the Xinjiang Uyghur Autonomous Region generates 4.67 tons of carbon per year [42]. The number of vehicles can be found in the Xinjiang Statistical Yearbook; E_{living} is the carbon emissions caused by each person's energy use. In the Xinjiang Uyghur Autonomous Region, one person is responsible for emitting about 5.84 tons of carbon per year [43]. Based on industrial output, vehicles, and population data from 2000 to 2020 (at 5-year intervals), linear regression was used to calculate industrial output, vehicles, and population in 2025 and 2030.

2.6. LULC Accuracy Verification

We compared the actual LULC data for 2015 and 2020 in the study area with the LULC data for the same years simulated based on the PLUS model, and then calculated the Kappa coefficient and overall accuracy (OA). The closer these two values are to 1, the higher the accuracy of the simulation; values greater than 0.8 indicate that the statistical accuracy of the model is satisfactory [25,29]. In this study, the Kappa coefficients of the simulated LULC for 2015 and 2020 were 0.931 and 0.905, respectively, and the overall accuracy was 0.964 and 0.949, respectively, indicating a high degree of confidence in the simulation results.

3. Results and Analysis

3.1. LULC Simulation under Multi-Scenarios

We applied the PLUS model to simulate the spatial distribution of land use in the Xinjiang region under different scenarios in 2025 and 2030, respectively, and calculated the dynamic rate of land change under four different scenarios for the two periods (Tables 3 and 4). The land use types in the Xinjiang region are dominated by bare land, this accounting for about 60.55% of the total study area. The LULC of the region also shows different trends in future scenarios, with the BAU scenario continuing the trend of urbanization in Xinjiang (Figure 3), with a dynamic land use index of 0.0045 and 0.0043 for construction in 2025 and 2030, respectively; this indicated land use change under this scenario is characterized by a slow, naturally expanding trend of construction. In the RED scenario, Xinjiang's construction expanded further, with land use dynamics of 0.0089 and 0.0145, respectively, in 2025 and 2030, corresponding to about 1.85% and 1.67% of other land types being converted to construction land (Figure 3); this indicates a more pronounced expansion of construction in the 2025–2030 period. Under this scenario, cropland also expands further, with land use dynamics of 0.0087 and 0.0095 in 2025 and 2030, respectively. Under the ELP scenario, the area of forest and grassland increases somewhat as a result of reforestation and ecological engineering policies, with about 7.28% and 0.57% of other land types converted to grassland in 2025 and 2030, respectively (Figure 3). In the SD scenario, we consider both the rapid economic development and the implementation of ecological projects to optimize the economic and ecological benefits. In this case, forest land increases by 554 km^2 and 2089 km^2 in 2025 and 2030, respectively, compared with 2020. There is a similar trend of construction land expansion, with an increase of 413.3 km^2 and 609.8 km^2 in the 2025 and 2030 SD scenarios, respectively, compared with 2020.

Table 3. LULC and its dynamic index K (%) in Xinjiang for each of the 2020–2025 scenarios.

LULC Type	Areal Coverage (km^2)					LULC Dynamic Index K (%)			
	2020	2025 BAU	2025 RED	2025 ELP	2025 SD	2020–2025 BAU	2020–2025 RED	2020–2025 ELP	2020–2025 SD
Cropland	90,255.7	93,594.9	94,215	86,520.5	90,956.1	0.007399	0.008774	−0.008277	0.001552
Forest	27,454.1	27,321.6	27,250	28,004.6	28,008.1	−0.00097	−0.001487	0.004010	0.004036
Grassland	48,4605	487,602	480,355	490,659	486,124	0.001237	−0.001754	0.002499	0.000627
Water	34,784.8	35,401.4	34,900.2	33,694.9	33,503.6	0.003545	0.000664	−0.006267	−0.007366
Constructed	9185.8	9393.3	9597.38	9314.3	9599.1	0.004518	0.008961	0.002798	0.008999
Bare land	992,105	985,077	992,073	989,940	989,942	−0.00142	−0.000006	−0.000436	−0.000436

Table 4. LULC and its dynamic index K (%) in Xinjiang for each of the 2020–2030 scenarios.

LULC Type	Areal Coverage (km^2)					LULC Dynamic Index K (%)			
	2025 BAU	2030 BAU	2030 RED	2030 ELP	2030 SD	2025 BAU–2030 BAU	2025 BAU–2030 RED	2025 BAU–2030 ELP	2025 BAU–2030 SD
Cropland	93,594.9	96,911.3	98,051.9	83,327.4	91,802	0.007087	0.009524	−0.021940	−0.003831
Forest	27,321.6	27,189.9	26,917.4	28,120.4	29,410.6	−0.000964	−0.002959	0.005847	0.015292
Grassland	487,602	490,577	476,350	496,092	489,906	0.001220	−0.004615	0.003482	0.000945
Water	35,401.4	36,013.8	35,011.7	34,974.5	34,784.3	0.003460	−0.002202	−0.002412	−0.003486
Constructed	9393.3	9599.2	10,074.6	9398	10,003.1	0.004384	0.014506	0.000100	0.012984
Bare land	985,077	978,099	991,985	986,479	982,485	−0.001417	0.001403	0.000285	−0.000526

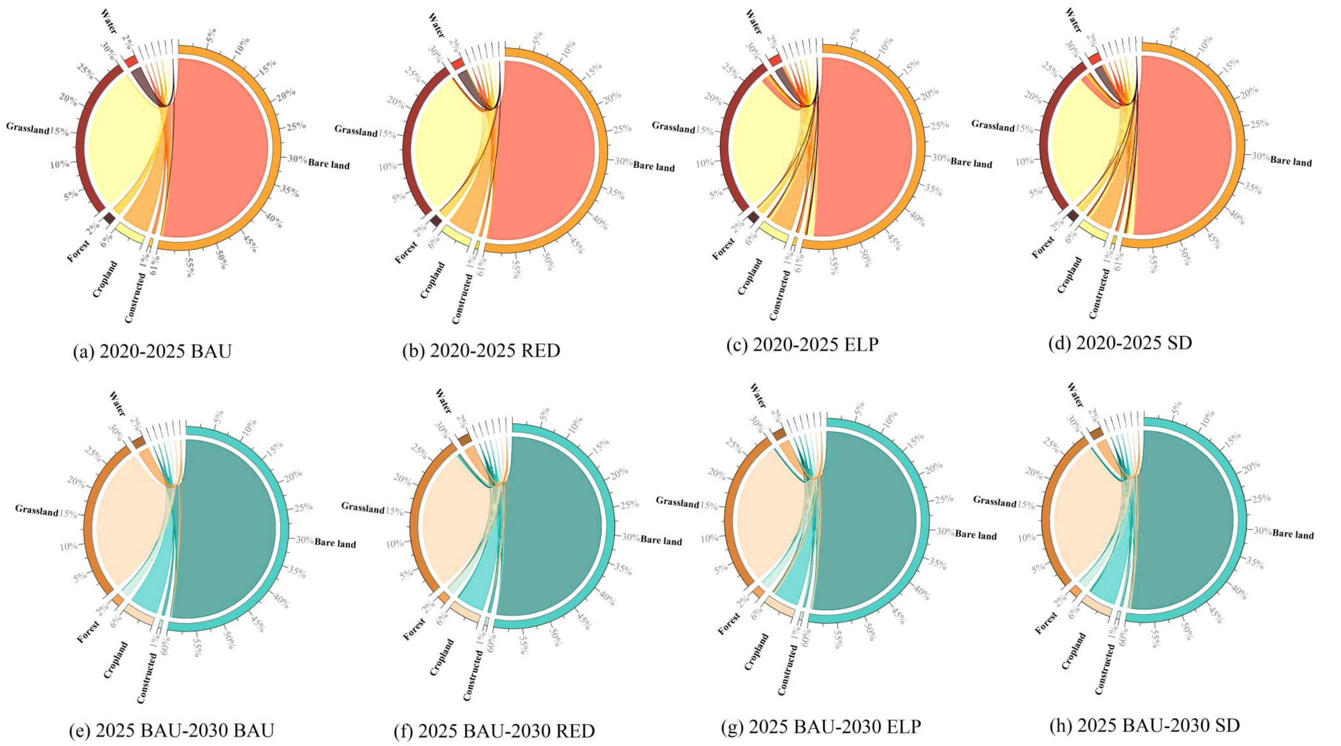

Figure 3. Transfer matrix of land use types under different land use scenarios in the Xinjiang region during different periods from 2020 to 2030. Where (**a**) is the land use transfer matrix for the 2020 to 2025 BAU scenario; (**b**) is the land use transfer matrix for the 2020 to 2025 RED scenario; (**c**) is the land use transfer matrix for the 2020 to 2025 ELP scenario; (**d**) is the land use transfer matrix for the 2020 to 2025 SD scenario; (**e**) is the land use transfer matrix for the 2025 BAU to 2030 BAU scenario; (**f**–**h**) and so on.

To explore the spatial and temporal characteristics of different land use types in Xinjiang under four future scenarios, we calculated the area of land use types during 2020–2030. Figure 4 shows the changes in the spatial patterns of cropland, forest land, grassland, and construction land in Xinjiang between 2020 and 2030 under the BAU, RED, ELP, and SD scenarios. Cropland significantly increased under the BAU, RED, and SD scenarios in 2025, increasing by 3339.2 km^2, 3959.3 km^2, and 700.4 km^2, respectively. These locations were mainly concentrated near the urban expansion zone along the northern slopes of the Tianshan Mountains, the Yili River Valley, the Aksu region, and the urban–rural farming belt in the Hotan region. In contrast, forest area decreased by 132.5 km^2 and 204.1 km^2 in 2025 under the BAU and RED scenarios, respectively, mainly in the Altai Mountains, the Yili River Valley, and the valley buffer zone near the Kunlun Mountains. By 2030, grassland under the RED scenario degraded extensively, with a decline of about 11,252 km^2, mainly in the Altai Mountains in the north, the Tianshan Mountains in the center, and near the Kunlun Mountains in the south of the study area, probably due to rapid urbanization at the expense of some forest and grassland. In addition, construction land shows an increasing trend in all four scenarios in 2030; the only difference is the magnitude of the increase, with the largest increases evidently occurring under the RED scenario, where the area increased by about 681.3 km^2, mainly in the urban agglomeration on the northern slopes of the Tianshan Mountains, the Aksu region, and the Kashgar region.

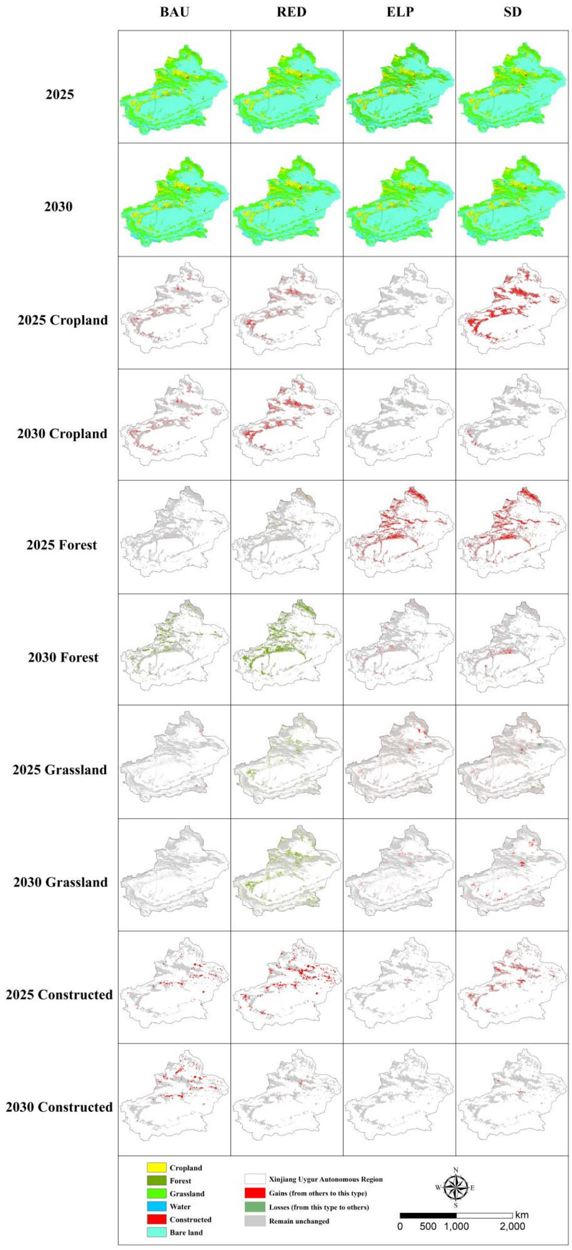

Figure 4. Changes in the spatiotemporal patterns of ecosystem types in each scenario from 2020 to 2030.

3.2. Spatial and Temporal Changes in the Supply of Carbon Sequestration under Different Scenarios

We used a random forest technique that incorporates environmental factors in our approach to assess changes in the landscape pattern of LULC-induced carbon sequestration service in terrestrial ecosystems in Xinjiang under different scenarios from 2020 to 2030 (Figure 5). The results show a clear spatial and temporal divergence in carbon sequestration under different scenarios. Under the BAU scenario in 2025, carbon sequestration shows a small annual increase compared to 2020 (interval of five years), of about 540 Tg. Under the RED scenario in 2025, carbon sequestration shows a decreasing trend compared to the BAU scenario, with an overall decrease of about 30 Tg, likely due to the continued expansion of construction driven by greater land use, resulting in the production of carbon from terrestrial ecosystems. In the 2025 SD scenario, carbon sequestration increased by another 370 Tg compared to the BAU scenario. This is because the SD scenario combines ecological and economic development, so the increase in forest and grassland areas leads to an increase in total carbon sequestration. In 2030, both the ELP and RED scenarios show an increase in carbon sequestration compared to the BAU scenario, by 20 Tg and 60 Tg, respectively. In the 2030 SD scenario, carbon sequestration increases significantly due to the pronounced profound expansion of forested grassland and the high carbon sequestration service capacity of forested land, making this scenario a carbon sink.

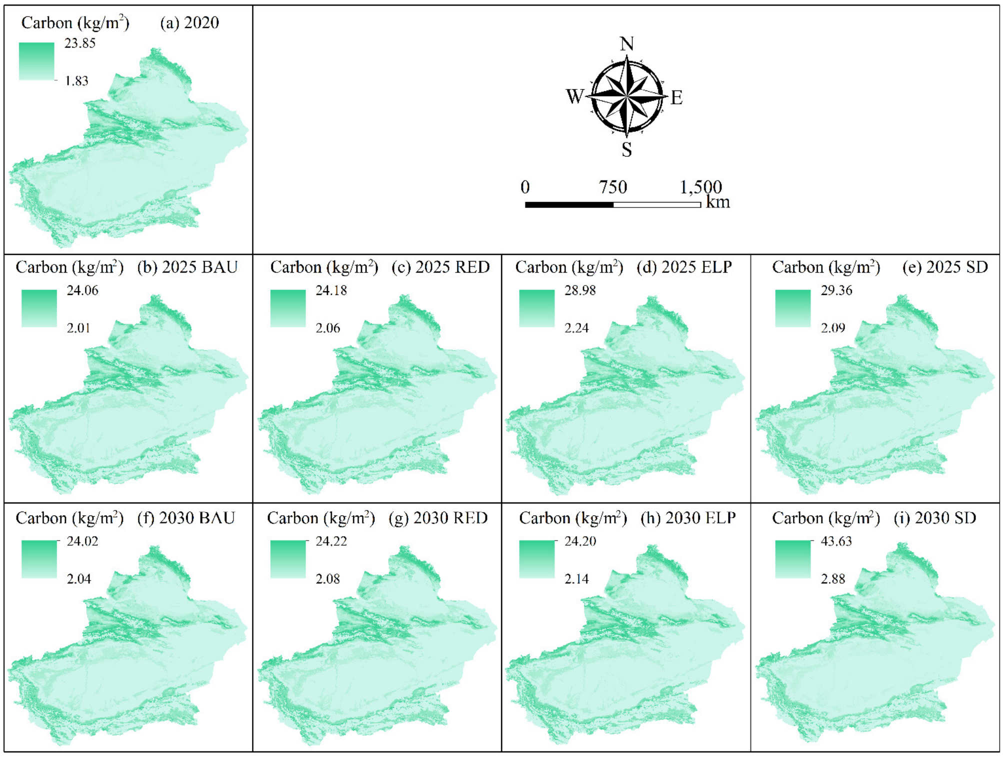

Figure 5. Spatial distribution characteristics of carbon sequestration service in each scenario during 2020–2030.

3.3. Analysis of the Supply and Demand for Carbon Sequestration under Different Future Scenarios

Xinjiang's carbon supply under different scenarios during 2020–2030 can hardly meet the current demand for carbon emissions (Figure 6), and the impact of land use on carbon supplies under different scenarios is also significant. In particular, the carbon supply in Xinjiang changes from 9.26 Pg in 2020 to 14.26 Pg under the SD scenario in 2030, while the carbon demand increases from 147.93 Pg in 2020 to 195.79 Pg, equivalent to an increase of about 32.35%. Considering the land use patterns under the different scenarios, the high-value areas of carbon stock are mainly distributed in the Altai Mountains, Tianshan Mountains, and Yili River Valley in the northern part of the study area due to the spatial distribution of forests and grasslands (Figure 6). Areas with low values of carbon sequestration service are distributed around bare land, construction land, and cultivated areas near river valley plains. Because of the high population density and industrialization of construction land, the carbon demand in this area is high, and the high-value areas of carbon demand are all concentrated around construction areas. In 2025 and 2030, in all the different scenarios for carbon sequestration in Xinjiang, the demand for a carbon sequestration service is exacerbated by the increasing expansion of construction areas, but the SD sustainability scenarios planned for this study can partly mitigate the deficit levels of carbon sequestration supply and demand.

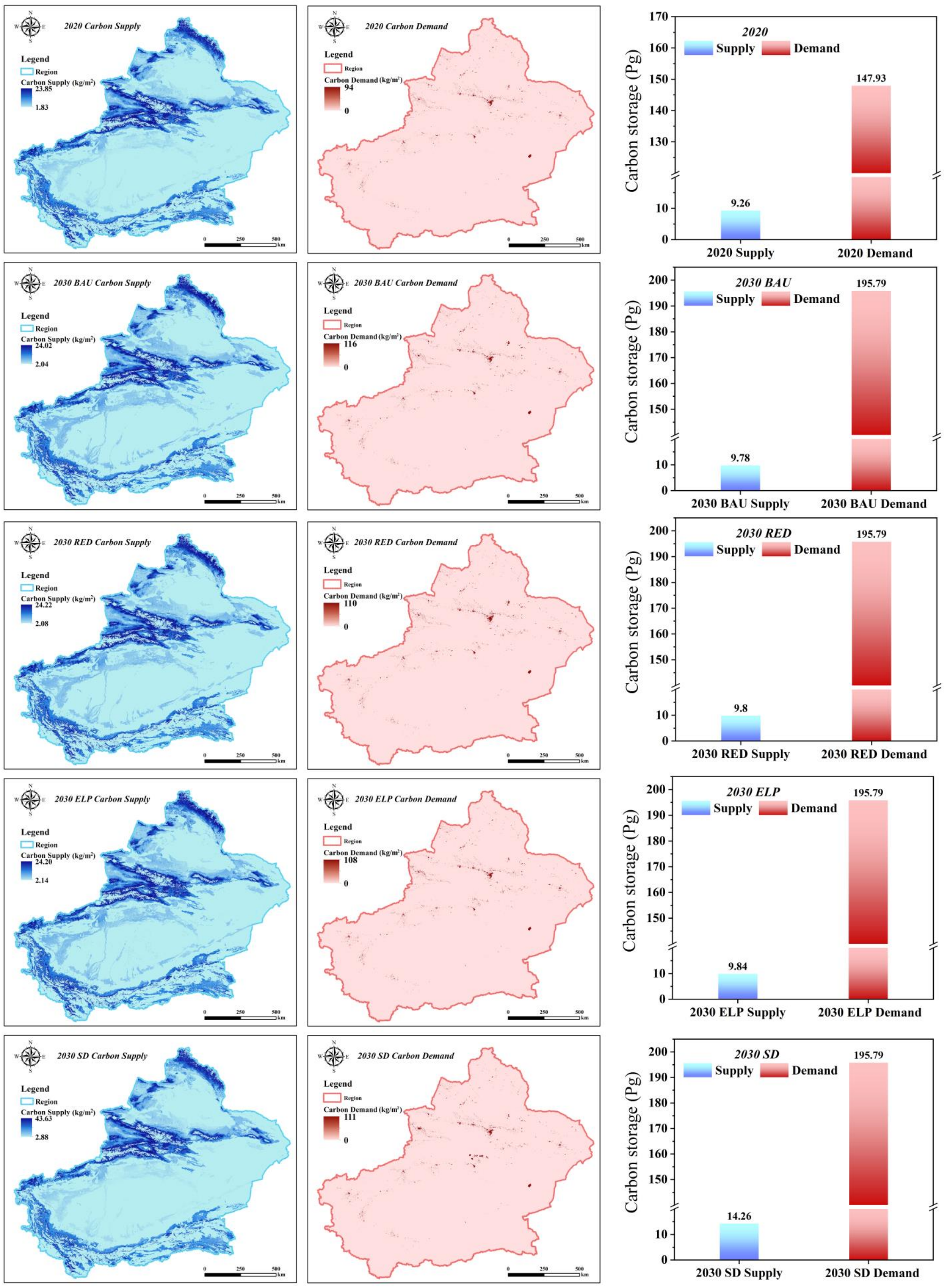

Figure 6. Spatial distribution of carbon stock supply and demand in Xinjiang under four different scenarios during 2020–2030.

4. Discussion

4.1. Analyses of Future Land Use Change under Different Scenarios

Based on the concept of sustainable development and the perspective of system evolution, this study proposes a land use evaluation framework for regional sustainable development that is oriented towards future development dynamics [44]. This study also attempts to apply global sustainable development goals at the local scale, which can effectively place regional development at the provincial level in the context of global sustainable development assessment and provide a basis for making decisions to help integrate regional development into the process of globalization. In addition, the United Nations Environment Program recognizes the key role of terrestrial ecosystem services in the SDGs, and in our study, we focus on terrestrial ecosystems, which echoes SDG 15.3 to combat desertification and restore degraded land and soil [35]. Land use planning is important for achieving SDG 15.3, and we should work towards a land-degradation-neutral world via better land use scenario planning. In addition, ecosystem services are central to achieving SDG 15.9 and should be integrated into national and local developmental processes [24,35,36].

To ensure the study's accuracy, we simulated the LULC data for 2015 and 2020 using the PLUS model, with Kappa coefficients of 0.931 and 0.905 and overall accuracies of 0.964 and 0.949, respectively, indicating a high degree of confidence in the simulation results. In addition, the PLUS model was used to simulate land use patterns in Xinjiang from 2020 to 2030 under four different scenarios, with a slight magnitude growth trend for cropland and construction land in the BAU scenario and a sharp expansion pattern in the RED scenario, both consistent with the findings of Fu et al. [33] in Xinjiang. In the ELP scenario, the large expansion of forests and grasslands was concentrated in the alpine forest–grassland and Yili River valley regions of the study area, which is also consistent with the findings of Shi et al. in the same valley [25]. We also found that the SD sustainability scenario accounts for the urbanization process while paying more attention to ecological protection, limiting the uncontrolled growth of urban space, and slowing down or even reversing the rising trend of constructed patches in some areas [35].

4.2. Analysis of the Impact of LULC on Carbon

This study completes the first high-resolution mapping of terrestrial ecosystem carbon sequestration in Xinjiang under different future scenarios. This fine-scale mapping shows that we can combine the contributions of nature and the needs of people [45]. Moreover, the RF approach applied in this study is superior to other methods for estimating carbon sequestration, and our carbon density raster data are spatially continuous rather than using the same carbon density value fixed for each land use type [20,21].

In addition, to ensure the accuracy of the study, we calibrated the output result parameters of Xinjiang carbon sequestration simulated by the RF model with the results of other studies on Xinjiang stocks. Via soil profiling, Yan et al. estimated the soil carbon stock in Xinjiang residing in a 0 to 100 cm depth to be about 19.56 Pg [46]. However, one study did find that the organic carbon in the top 20 cm of soils in Xinjiang accounts for 37.9% of the percentage of organic carbon in a 1 m deep soil layer [47]. Therefore, Yan et al. estimated the carbon stock in the topsoil layer of Xinjiang to be about 7.41 Pg, whereas this study estimated a higher carbon stock of terrestrial ecosystems in Xinjiang, at about 9.26 Pg. This discrepancy may be because we modeled not only the soil carbon sequestration service but also the aboveground and belowground biomass carbon sequestration, this being a plausible explanation for the relatively high results of our study.

4.3. Analysis of the Supply and Demand of the Carbon Sequestration Service in Different Scenarios

Studies have shown that LULC is considered a key anthropogenic driver of ecosystem service change at the regional scale [48,49]. Our study used measured datasets of aboveground biomass carbon density, belowground biomass carbon density, and soil carbon density, combined with a random forest model and spatial mapping of raster layers of different future land uses, as factorial environmental variables [17]. In this way, we proposed a new scheme for the spatial simulation of the terrestrial ecosystem carbon sequestration service with the GMOP-PLUS model combined with the random forest method.

According to our findings, the ELP and SD scenarios of this study simulated the implementation of ecological projects, whose primary aim is restoring forests and protecting grasslands, mainly to prevent increased desertification and soil erosion in Xinjiang, and to increase the productivity of vegetation for more carbon sequestration service, objectives closely related to dozens of ecological projects carried out in China in the last half-century [9]. Furthermore, our study shows that the growth of one land use patch comes at the cost of the decline of another land use type. For example, in the RED scenario, the growth of built-upon land comes at the expense of forested grassland [23,31,50]. We expect the supply of carbon storage in Xinjiang to increase by about 5.72% in 2020, but, at the same time, the demand will rise by 21.80%. In 2030, this supply and demand servicing will intensify the deficit. Xinjiang's supply of carbon stock in 2030 will increase by approximately 5.61% compared to 2020, yet the demand for it will increase by 32.35% in the meantime. Still, in the SD scenario, our projections can serve to mitigate some of the carbon sources through the implementation of ecological engineering projects, and the different scenarios are set up to help clarify the relationship between different LULC structures and ESs carbon stock. For example, in the 2025 RED scenario, the increase in carbon sequestration services from cropland expansion is about 12.61 Mg, while in 2030 this trend is reversed and carbon sourcing occurs, with a cumulative net release of 2.42 Mg. Alternatively, in the 2025 SD scenario, cropland expansion is expected to generate a carbon sink of 63.26 Mg, while in 2030 this trend is slowed down, with a projected net carbon sequestration of 11.24 Mg. This result is likely attributed to the expectation that cropland will reach an expansion saturation in 2030 in the scenario simulation setting so that cropland expansion is eventually slowed down. Our findings suggest that different scenarios can help clarify the relationship between different LULC structures and ESs carbon sequestration.

4.4. Limitations and Perspectives

In this study, future land use patterns under different scenarios were generated through the PLUS model, and carbon stock supply and demand services were assessed for various scenarios. However, there are still some uncertainties and limitations. For example, this study only portrayed four different future scenarios of LULC through policy guidelines; the four alternative scenarios do not represent all possible LULC realities, and more comprehensive scenarios should be explored in subsequent studies. For example, the impact of future climate change on LULC could be considered, among others, to address multi-stakeholder needs for optimal land use policies [25,51].

In addition, with the development of low carbon technologies and the policy direction of the national dual carbon targets, whether future carbon demand will still develop in line with the original demand trend to address the need to achieve China's peak carbon policy by 2030 could potentially impact the results of the carbon stock demand component. Therefore, future studies should plan the LULC scenarios more rationally and truly consider the future carbon stock demand in the context of China's policy. This will help provide better scientific references for future regional decision-making and sustainable development planning.

5. Conclusions

In this study, we coupled the gray multi-objective optimization (GMOP) and patch generation land use simulation (PLUS) models and proposed a new SD sustainability scenario framework for optimizing the structure of future land use in Xinjiang by using the GMOP-PLUS model. This work also explores the carbon sequestration services of terrestrial ecosystems in key regions from the perspective of land use change, and addresses the disparities arising between the supply and demand of carbon sequestration services in

Xinjiang in the future years of 2025 and 2030. The starkest findings to emerge from this study are as follows: (1) the future expansion of arable land in Xinjiang will occur at the expense of some forest and grassland areas, which are particularly prominent in the interlocking zones of river valleys and plains, especially in the Ili Valley, the Altay Mountains, etc.; (2) the supply and demand of carbon stock in Xinjiang will increase in 2025, but the demand is much greater than the supply, and in 2030 this supply and demand imbalance is exacerbated; and (3) Xinjiang, in the context of future cropland expansion, could alleviate the supply and demand deficit situation threatening Xinjiang's carbon stock; the occurrence of this mitigation is most likely under in the SD scenario. Nonetheless, some of the carbon sources can be mitigated by the implementation of ecological engineering in our planned SD scenario, and the analysis of the SD scenario and other scenarios can help to clarify the relationship between different LULC structures and carbon sequestration. Therefore, local governments can increase their efforts to protect ecosystem carbon sequestration services through policies such as returning farmland to forest, reasonable ecological land regulation, and appropriate afforestation activities, in addition to sequestering carbon belowground, while minimizing the loss of ecosystem service functions, to achieve the sustainable development of agroecology in key areas along the Belt and Road.

Author Contributions: H.W. and P.J. were responsible for the research design, analysis, and the manuscript's design and its review. M.S. drafted the manuscript and was responsible for data preparation, experiments, and analyses. W.S. was responsible for the research design and reviewing the manuscript. Resources and funding were procured by H.W. and P.J. M.Z., Z.L., K.Z. have performed the data processing work. L.Z., H.Z., X.F. performed the manuscript editing. T.D., M.F.B. performed the manuscript proofreading and retouching. All authors have read and agreed to the published version of the manuscript.

Funding: This research was financially supported by Major Science and Technology Special Projects in Xinjiang Uygur Autonomous Region, China (Integrated demonstration of high quality, high yield and high efficiency standardized production technology for cotton, No. 2020A01002).

Institutional Review Board Statement: Not applicable.

Informed Consent Statement: Written informed consent has been obtained from the patient(s) to publish this paper.

Data Availability Statement: The data presented in this study are available on request from the corresponding author.

Acknowledgments: Special thanks go to the College of Resources and Environment, University of Chinese Academy of Sciences, for supporting the implementation of this study. We thank Xiaozhen Wang at the Northwest A&F University for her constructive suggestions. We also thank the anonymous reviewers for their constructive comments on the manuscript.

Conflicts of Interest: The authors declare no conflict of interest.

References

1. Wang, Y.; Wang, X.; Wang, K.; Chevallier, F.; Zhu, D.; Lian, J.; He, Y.; Tian, H.; Li, J.; Zhu, J. The size of the land carbon sink in China. *Nature* **2022**, *603*, E7–E9. [CrossRef] [PubMed]
2. Liu, C.; Liang, Y.; Zhao, Y.; Liu, S.; Huang, C. Simulation and Analysis of the Effects of Land Use and Climate Change on Carbon Dynamics in the Wuhan City Circle Area. *Int. J. Environ. Res. Public Health* **2021**, *18*, 11617. [CrossRef] [PubMed]
3. Tang, X.; Zhao, X.; Bai, Y.; Tang, Z.; Wang, W.; Zhao, Y.; Wan, H.; Xie, Z.; Shi, X.; Wu, B. Carbon pools in China's terrestrial ecosystems: New estimates based on an intensive field survey. *Proc. Natl. Acad. Sci. USA* **2018**, *115*, 4021–4026. [CrossRef] [PubMed]
4. Eggleston, H.; Buendia, L.; Miwa, K.; Ngara, T.; Tanabe, K. *2006 IPCC Guidelines for National Greenhouse Gas Inventories*; U.S. Department of Energy Office of Scientific and Technical Information: Oak Ridge, TN, USA, 2006.
5. Houghton, R. The annual net flux of carbon to the atmosphere from changes in land use 1850–1990. *Tellus B* **1999**, *51*, 298–313. [CrossRef]
6. Jiang, H.; Peng, J.; Dong, J.; Zhang, Z.; Xu, Z.; Meersmans, J. Linking ecological background and demand to identify ecological security patterns across the Guangdong-Hong Kong-Macao Greater Bay Area in China. *Landsc. Ecol.* **2021**, *36*, 2135–2150. [CrossRef]

7. Schwartz, C.; Shaaban, M.; Bellingrath-Kimura, S.D.; Piorr, A. Participatory Mapping of Demand for Ecosystem Services in Agricultural Landscapes. *Agriculture* **2021**, *11*, 1193. [CrossRef]
8. Li, H.; Wu, Y.; Liu, S.; Xiao, J.; Zhao, W.; Chen, J.; Alexandrov, G.; Cao, Y. Decipher soil organic carbon dynamics and driving forces across China using machine learning. *Glob. Chang. Biol.* **2022**, *28*, 3394–3410. [CrossRef] [PubMed]
9. Zhao, M.; He, Z.; Du, J.; Chen, L.; Lin, P.; Fang, S. Assessing the effects of ecological engineering on carbon storage by linking the CA-Markov and InVEST models. *Ecol. Indic.* **2019**, *98*, 29–38. [CrossRef]
10. Stockmann, U.; Adams, M.A.; Crawford, J.W.; Field, D.J.; Henakaarchchi, N.; Jenkins, M.; Minasny, B.; McBratney, A.B.; De Courcelles, V.d.R.; Singh, K. The knowns, known unknowns and unknowns of sequestration of soil organic carbon. *Agric. Ecosyst. Environ.* **2013**, *164*, 80–99. [CrossRef]
11. Wieder, W.R.; Bonan, G.B.; Allison, S.D. Global soil carbon projections are improved by modelling microbial processes. *Nat. Clim. Chang.* **2013**, *3*, 909–912. [CrossRef]
12. Nayak, A.K.; Rahman, M.M.; Naidu, R.; Dhal, B.; Swain, C.K.; Nayak, A.D.; Tripathi, R.; Shahid, M.; Islam, M.R.; Pathak, H. Current and emerging methodologies for estimating carbon sequestration in agricultural soils: A review. *Sci. Total Environ.* **2019**, *665*, 890–912. [CrossRef] [PubMed]
13. Fensholt, R.; Sandholt, I.; Rasmussen, M.S.; Stisen, S.; Diouf, A. Evaluation of satellite based primary production modelling in the semi-arid Sahel. *Remote Sens. Environ.* **2006**, *105*, 173–188. [CrossRef]
14. Zhao, M.; Running, S.W.; Nemani, R.R. Sensitivity of Moderate Resolution Imaging Spectroradiometer (MODIS) terrestrial primary production to the accuracy of meteorological reanalyses. *J. Geophys. Res. Biogeosci.* **2006**, *111*, G1. [CrossRef]
15. Rahman, A.; Sims, D.A.; Cordova, V.D.; El-Masri, B.Z. Potential of MODIS EVI and surface temperature for directly estimating per-pixel ecosystem C fluxes. *Geophys. Res. Lett.* **2005**, *32*, 19. [CrossRef]
16. Scharlemann, J.P.; Tanner, E.V.; Hiederer, R.; Kapos, V. Global soil carbon: Understanding and managing the largest terrestrial carbon pool. *Carbon Manag.* **2014**, *5*, 81–91. [CrossRef]
17. Zhang, M.; Shi, W.; Xu, Z. Systematic comparison of five machine-learning models in classification and interpolation of soil particle size fractions using different transformed data. *Hydrol. Earth Syst. Sci.* **2020**, *24*, 2505–2526. [CrossRef]
18. Euliss, N.H., Jr.; Smith, L.M.; Liu, S.; Feng, M.; Mushet, D.M.; Auch, R.F.; Loveland, T.R. The need for simultaneous evaluation of ecosystem services and land use change. *Environ. Sci. Technol.* **2010**, *44*, 7761–7763. [CrossRef]
19. Maring, L.; Blauw, M. Asset management to support urban land and subsurface management. *Sci. Total Environ.* **2018**, *615*, 390–397. [CrossRef] [PubMed]
20. Goldstein, J.H.; Caldarone, G.; Duarte, T.K.; Ennaanay, D.; Hannahs, N.; Mendoza, G.; Polasky, S.; Wolny, S.; Daily, G.C. Integrating ecosystem-service tradeoffs into land-use decisions. *Proc. Natl. Acad. Sci. USA* **2012**, *109*, 7565–7570. [CrossRef] [PubMed]
21. Nelson, E.; Mendoza, G.; Regetz, J.; Polasky, S.; Tallis, H.; Cameron, D.; Chan, K.M.; Daily, G.C.; Goldstein, J.; Kareiva, P.M. Modeling multiple ecosystem services, biodiversity conservation, commodity production, and tradeoffs at landscape scales. *Front. Ecol. Environ.* **2009**, *7*, 4–11. [CrossRef]
22. Zhang, D.; Huang, Q.; He, C.; Yin, D.; Liu, Z. Planning urban landscape to maintain key ecosystem services in a rapidly urbanizing area: A scenario analysis in the Beijing-Tianjin-Hebei urban agglomeration, China. *Ecol. Indic.* **2019**, *96*, 559–571. [CrossRef]
23. Li, Z.; Cheng, X.; Han, H. Future impacts of land use change on ecosystem services under different scenarios in the ecological conservation area, Beijing, China. *Forests* **2020**, *11*, 584. [CrossRef]
24. Wu, X.; Fu, B.; Wang, S.; Song, S.; Li, Y.; Xu, Z.; Wei, Y.; Liu, J. Decoupling of SDGs followed by re-coupling as sustainable development progresses. *Nat. Sustain.* **2022**, *5*, 452–459. [CrossRef]
25. Shi, M.; Wu, H.; Fan, X.; Jia, H.; Dong, T.; He, P.; Baqa, M.F.; Jiang, P. Trade-offs and synergies of multiple ecosystem services for different land use scenarios in the yili river valley, China. *Sustainability* **2021**, *13*, 1577. [CrossRef]
26. Wang, X.; Dong, X.; Liu, H.; Wei, H.; Fan, W.; Lu, N.; Xu, Z.; Ren, J.; Xing, K. Linking land use change, ecosystem services and human well-being: A case study of the Manas River Basin of Xinjiang, China. *Ecosyst. Serv.* **2017**, *27*, 113–123. [CrossRef]
27. Chen, J.; Jiang, B.; Bai, Y.; Xu, X.; Alatalo, J.M. Quantifying ecosystem services supply and demand shortfalls and mismatches for management optimisation. *Sci. Total Environ.* **2019**, *650*, 1426–1439. [CrossRef]
28. Xu, L.; He, N.; Yu, G. A dataset of carbon density in Chinese terrestrial ecosystems (2010s). *China Sci. Data* **2019**, *4*, 49–54.
29. Liang, X.; Guan, Q.; Clarke, K.C.; Liu, S.; Wang, B.; Yao, Y. Understanding the drivers of sustainable land expansion using a patch-generating land use simulation (PLUS) model: A case study in Wuhan, China. *Comput. Environ. Urban Syst.* **2021**, *85*, 101569. [CrossRef]
30. Wang, Y.; Li, X.; Zhang, Q.; Li, J.; Zhou, X. Projections of future land use changes: Multiple scenarios-based impacts analysis on ecosystem services for Wuhan city, China. *Ecol. Indic.* **2018**, *94*, 430–445. [CrossRef]
31. Li, C.; Wu, Y.; Gao, B.; Zheng, K.; Wu, Y.; Li, C. Multi-scenario simulation of ecosystem service value for optimization of land use in the Sichuan-Yunnan ecological barrier, China. *Ecol. Indic.* **2021**, *132*, 108328. [CrossRef]
32. Zhang, H.-B.; Zhang, X.-H. Land use structural optimization of Lilin based on GMOP-ESV. *Trans. Nonferrous Met. Soc. China* **2011**, *21*, s738–s742. [CrossRef]
33. Fu, Q.; Hou, Y.; Wang, B.; Bi, X.; Li, B.; Zhang, X. Scenario analysis of ecosystem service changes and interactions in a mountain-oasis-desert system: A case study in Altay Prefecture, China. *Sci. Rep.* **2018**, *8*, 12939. [CrossRef] [PubMed]

34. Liang, J.; Li, S.; Li, X.; Li, X.; Liu, Q.; Meng, Q.; Lin, A.; Li, J. Trade-off analyses and optimization of water-related ecosystem services (WRESs) based on land use change in a typical agricultural watershed, southern China. *J. Clean. Prod.* **2021**, *279*, 123851. [CrossRef]
35. Peng, K.; Jiang, W.; Ling, Z.; Hou, P.; Deng, Y. Evaluating the potential impacts of land use changes on ecosystem service value under multiple scenarios in support of SDG reporting: A case study of the Wuhan urban agglomeration. *J. Clean. Prod.* **2021**, *307*, 127321. [CrossRef]
36. Giuliani, G.; Mazzetti, P.; Santoro, M.; Nativi, S.; Van Bemmelen, J.; Colangeli, G.; Lehmann, A. Knowledge generation using satellite earth observations to support sustainable development goals (SDG): A use case on Land degradation. *Int. J. Appl. Earth Obs. Geoinf.* **2020**, *88*, 102068. [CrossRef]
37. Xinjiang Statistical Yearbook. 2020. Available online: http://www.stats.gov.cn/tjsj./ndsj/ (accessed on 1 May 2022).
38. Xie, G.; Zhang, C.; Zhang, C.; Xiao, Y.; Lu, C. The value of ecosystem services in China. *Resour. Sci.* **2015**, *37*, 1740–1746.
39. Breiman, L. Bagging predictors. *Mach. Learn.* **1996**, *24*, 123–140. [CrossRef]
40. Sun, Y.; Zhang, S.; Tao, F.; Aboelenein, R.; Amer, A. Improving Winter Wheat Yield Forecasting Based on Multi-Source Data and Machine Learning. *Agriculture* **2022**, *12*, 571. [CrossRef]
41. Xu, L.; Yu, G.; He, N.; Wang, Q.; Gao, Y.; Wen, D.; Li, S.; Niu, S.; Ge, J. Carbon storage in China's terrestrial ecosystems: A synthesis. *Sci. Rep.* **2018**, *8*, 2806. [CrossRef]
42. Li, Y.; Qian, Y. An analysis of operation cost of Chinese family car. *Market Res.* **2008**, *1*, 52–54.
43. Cai, H. *Factors of Northern and Southern China per Capita CO_2 Emission in China's Household*; Jinan University: Guangzhou, China, 2016. (In Chinese)
44. Eustachio, J.H.P.P.; Caldana, A.C.F.; Liboni, L.B.; Martinelli, D.P. Systemic indicator of sustainable development: Proposal and application of a framework. *J. Clean. Prod.* **2019**, *241*, 118383. [CrossRef]
45. Chaplin-Kramer, R.; Sharp, R.P.; Weil, C.; Bennett, E.M.; Pascual, U.; Arkema, K.K.; Brauman, K.A.; Bryant, B.P.; Guerry, A.D.; Haddad, N.M. Global modeling of nature's contributions to people. *Science* **2019**, *366*, 255–258. [CrossRef] [PubMed]
46. Yan, A. *Spatial Distribution and Storages Estimation of Soil Organic Carbon and Soil Inorganic Carbon in Xinjiang, China*; China Agricultural University: Beijing, China, 2015. (In Chinese)
47. Wang, X.; Yang, D.; Xiong, H. Characteristics of soil organic carbon under different vegetation types in Xinjiang. *Arid. Zone Res.* **2017**, *34*, 782–788.
48. Bai, Y.; Wong, C.P.; Jiang, B.; Hughes, A.C.; Wang, M.; Wang, Q. Developing China's Ecological Redline Policy using ecosystem services assessments for land use planning. *Nat. Commun.* **2018**, *9*, 3034. [CrossRef]
49. Fu, B.; Zhang, L.; Xu, Z.; Zhao, Y.; Wei, Y.; Skinner, D. Ecosystem services in changing land use. *J. Soils Sediments* **2015**, *15*, 833–843. [CrossRef]
50. Chen, Y.; Zhang, L.; He, L.; Men, M. Multi-scenario simulation of land use structure based on dual combined models. *Acta Ecol. Sin.* **2016**, *36*, 5391–5400.
51. Wang, Y.; Huang, M.; Wang, X. Impacts of land use and climate change on agricultural productivity in Shanghai. *Acta Sci. Circumstantiae* **2010**, *30*, 641–648.